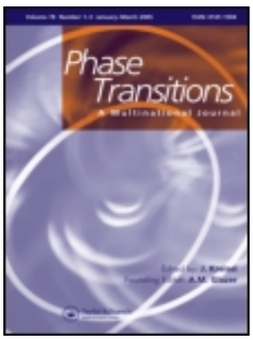

Taylor & Francis
Taylor & Francis Group

Phase Transitions
A Multinational Journal

ISSN: 0141-1594 (Print) 1029-0338 (Online) Journal homepage: https://www.tandfonline.com/loi/gpht20

Monitoring the gelation of polyacrylamide–sodium alginate composite by fluorescence technique

Gülşen Akın Evingür , Filiz Tezcan , F. Bedia Erim & Önder Pekcan

To cite this article: Gülşen Akın Evingür , Filiz Tezcan , F. Bedia Erim & Önder Pekcan (2012) Monitoring the gelation of polyacrylamide–sodium alginate composite by fluorescence technique, Phase Transitions, 85:6, 530-541, DOI: 10.1080/01411594.2011.629363

To link to this article: https://doi.org/10.1080/01411594.2011.629363

Phase Transitions
Vol. 85, No. 6, June 2012, 530–541

Taylor & Francis
Taylor & Francis Group

Monitoring the gelation of polyacrylamide–sodium alginate composite by fluorescence technique

Gülşen Akın Evingür[a], Filiz Tezcan[b], F. Bedia Erim[b] and Önder Pekcan[c]*

[a]*Faculty of Science and Letters, Piri Reis University, 34940 Tuzla-İstanbul, Turkey;*
[b]*Faculty of Science and Letters, İstanbul Technical University, 34469 Maslak-İstanbul, Turkey;*
[c]*Faculty of Science and Letters, Kadir Has University, 34083 Cibali-İstanbul, Turkey*

(*Received 9 August 2011; final version received 2 October 2011*)

Polyacrylamide (PAAm)–sodium alginate (SA) composite was prepared with different amounts of SA varying in the range between 0.06% and 2% (w/v). The PAAm–SA composite was characterized by the steady-state fluorescence technique. Pyranine was added as a fluoroprobe for monitoring the polymerization. It was observed that pyranine molecules bind to AAm and SA chains upon the initiation of the polymerization. Thus, the fluorescence spectra of the bonded pyranines shift to the shorter wavelengths. Fluorescence spectra from the bonded pyranines allowed us to monitor the sol–gel phase transition, and to test the universality of the sol–gel transition as a function of SA contents. Observations around the critical point show that the gel fraction exponent, β, and the weight average degree of polymerization exponent, γ, agreed with the percolation result for (<0.25% (w/v)) SA contents. However, classical results were produced at (<2% (w/v)) SA contents.

Keywords: sodium alginate; acrylamide; universality; critical phenomena; fluorescence

1. Introduction

A composite can be defined as a substance composed of two or more materials with different base structures combined in such a way that the end product has properties different from either of the parent materials. Chemical gels doped with biological gels are a new class of composite materials. Polyacrylamide (PAAm) hydrogels are mainly produced by free radical cross-linking copolymerization of AAm in the presence of *N*,*N*′-methylenebis (acrylamide) (BIS) as the crosslinker. Since the monomers are solid at the polymerization temperature, the reactions are necessarily carried out in an aqueous solution of the monomers. On the other hand, alginates are linear polymers containing beta-(1-4)-linked D-mannuronic acid (M) and alfa-(1-4)-linked L-guluronic acid (G) residues of widely varying composition and sequence [1–3]. Alginate is considered as biocompatible and a hydrogel easy to form by divalent cations. Alginate hydrogel has been

*Corresponding author. Email: pekcan@khas.edu.tr

ISSN 0141–1594 print/ISSN 1029–0338 online

http://dx.doi.org/10.1080/01411594.2011.629363
http://www.tandfonline.com

intensively studied for cell encapsulation, cell transplantation and tissue investigations concerned the critical phenomenon of the sol–gel transition in aqueous alginate solutions.

Graft copolymers of sodium alginate (SA) with acrylamide have been characterized by viscometer, IR spectroscopy, SEM, and XRD study [3]. The sol–gel transition was monitored by measuring the dynamic mechanical spectroscopy [4], UV-Vis spectrophotometry [5], molar ratio [6], and rheology methods [7]. The critical exponents were evaluated and the structure self-similarity was found in the critical gel for each method. Alginate microspheres were prepared by internal gelation [8]. Development and effect on insulin stability were investigated. Synthesis, gelation, and swelling characterizations of SA/acrylamide semi-interpenetrating polymer networks were performed by thermal and elasticity analysis [9,10] for the some textile dyes [11].

Experimental techniques used for monitoring sol–gel transition must be very sensitive to the structural changes, and should not mechanically disturb the system. Fluorescence technique is particularly useful for elucidation of detailed structural aspects of the gels. This technique is based on the interpretation of the change in anisotropy, emission and/or excitation spectra, emission intensity, and viewing the lifetimes of injected aromatic molecules to monitor the change in their microenvironment [12–14]. Fluorescence probes can be used for the studies on polymerization and gelation. By adding a luminescent dye as a probe, it is possible to measure some physical parameters of the polymerizing system, such as polarity [15,16], physical aging [17], mobility [18], and viscosity [19]. Recent studies in our laboratory, using pyranine as an intrinsic fluoroprobe, showed that the universality of composite gels could be described by classical and percolation exponents during the sol–gel phase transition in PAAm-kappa(κ)-carrageenan [20], PAAm–PNIPA [21], and PAAm-multiwalled carbon nanotube composites (MWNTs) [22]. In composite hydrogels, it is found that the critical exponents did not follow the features of the same universality class, where the most important factor is the monomer content in which the exponents drastically differ from percolation to the classical values. First, observations around the critical point show that the gel fraction exponent β agreed with the percolation result for low kappa(κ)-carrageenan contents (<2.0%). However, classical results were produced at high kappa(κ)-carrageenan contents (>2.0%) for PAAm-kappa(κ)-carrageenan composite system [20]. Second, the gel point of PAAm–PNIPA composites shows that the gel fraction exponent β agreed with the percolation result [21]. Third, the gel point, t_{gel}, for PAAm-MWNTs composite gels showed that the gel fraction exponent β agreed with the percolation result.

In this study, we aimed to study the gelation of AAm–SA composites and determined the gel fraction exponent, β and the weight average degree of polymerization exponent, γ, for this composite system. For this purpose, the aqueous solutions of AAm and SA mixtures were prepared. The total monomer content of AAm was kept at 2 M in all solutions and SA concentrations changed between 0.06% and 2% (w/v). Pyranine added to the pre-polymerization solution presented a spectral shift to the shorter wavelengths upon the initiation of polymerization. This spectral shift is due to the binding of pyranine to the polymer chains during the PAAm–SA composite polymerization. The pyranine, thus, becomes an intrinsic fluoroprobe, while it is extrinsic at the beginning of the reaction. The fluorescence intensity of the pyranine bonded to the strands of the composites allows one to directly measure the gel fraction and average degree of polymerization near the sol–gel phase transition. The percolation result for <0.25% (w/v) SA contents were noted. However, classical results were produced for <2% (w/v) SA contents and also the gelation time, t_{gel}, increased as SA contents were increased.

2. Theory

Hydrogels have received considerable attention with regard to the sol–gel phase transition process. The exact solution of the sol–gel phase transition was first given by Flory and Stockmayer [23–27] on a special lattice called Bethe lattice on which the closed loops were ignored. An alternative to the chemical-kinetic theory is the lattice percolation model [28,29] where monomers are thought to occupy the sites of a periodic lattice. A bond between these lattice sites is randomly formed with probability p. For a certain bond content p_c, defined as the percolation threshold, the infinite cluster starts to form in the thermodynamic limit. This is called the percolation cluster in polymer language. The polymeric system is in the sol state below the percolation threshold, p_c.

The predictions of these two theories about the critical exponents for the sol–gel phase transition are different from the point of the universality. Consider, for example, the exponents γ and β for the weight average degree of polymerization, DP_w, and the gel fraction G (average cluster size, S_{av}, and the strength of the infinite network P_∞ in percolation language) near the percolation threshold, are defined as,

$$DP_w \propto (p_c - p)^{-\gamma} \quad p \to p_c^- \tag{1}$$

$$G \propto (p - p_c)^{\beta} \quad p \to p_c^+ \tag{2}$$

where the Flory–Stockmayer theory (so-called the classical or mean-field theory) gives $\beta = \gamma = 1$, independent of the dimensionality while the percolation studies based on computer simulations give γ and β around 1.7 and 0.43 in three dimensions [28,29].

These two universality classes for gelation problem are separated by a Ginzburg criterion [30] that depends upon the chain length N between the branch points as well as the content of the non-reacting solvent. The vulcanization of long linear polymer chains (large N) belongs to the mean-field class. Critical percolation (small N) describes the polymerization of small multifunctional monomers [28,29,31,32].

Here, one would like to argue that the total fluorescence intensity from the bonded pyranines monitors the weight average degree of polymerization and the growing gel fraction for the cases below and above the gel point, respectively. This proportionality can easily be proven using a Stauffer-type argument [29], given as follows, under the assumption that the monomers occupy the sites of an imaginary periodic lattice.

The probability that a site belongs to a cluster of size s is given by $n_s \cdot s$, where n is the number of *s-clusters* (number of clusters including s sites) per lattice site. The probability that an arbitrary site belongs to any cluster is p is simply the probability that an arbitrary site is occupied. Thus, the probability, w_s that the cluster to which an arbitrary occupied site belongs contains exactly s site is,

$$w_s = \frac{n_s \cdot s}{\sum_s n_s \cdot s} \tag{3}$$

and thus the average cluster size, S is calculated by the following relation [28,29,31,32]

$$S = \sum_s w_s \cdot s = \frac{\sum n_s \cdot s^2}{\sum n_s \cdot s} \tag{4}$$

The definition of the average cluster size is the same for all dimensions, although n_s cannot be exactly calculated in higher dimensions [29]. This definition also holds for the bond percolation.

Now, let N_p be the number of pyranine molecules and N_m the other molecules (AAm, SA, BIS, APS, and water) in the lattice. Thus, the total lattice site, N, will be equal to $N_p + N_m$. The probability, P_p, that an arbitrary site is occupied by a pyranine molecule is simply N_p/N. The probability, P_y, that an arbitrary site is a pyranine and also belongs to the s-cluster can be calculated as a product of w_s and P_p,

$$P_y = P_p \cdot w_s = \frac{P_p \cdot n_s \cdot s}{\sum n_s \cdot s} \tag{5}$$

Thus, $P_y \cdot s$ will be the total number of pyranine molecules in each cluster including s sites. The total fluorescence intensity, I, which is proportional to the total number of pyranines trapped in the finite clusters, can be calculated as a summation over all s-clusters

$$I \sim \sum_s P_y \cdot s = \sum_s \frac{P_p \cdot n_s.s}{\sum n_s \cdot s} \cdot s = \frac{\sum P_p \cdot n_s \cdot s^2}{\sum n_s \cdot s} \tag{6}$$

where P_p can be taken out of the summation since the content of the pyranine is kept fixed for our studies,

$$I \sim P_p \frac{\sum n_s \cdot s^2}{\sum n_s \cdot s} = P_p \cdot S \tag{7}$$

Thus, the last expression shows that the total normalized fluorescent intensity, I, is proportional to the average cluster size S. Note that the proportionality factor, P_p, is simply the fraction of the pyranine molecules in the sample cell. Intensity will be linearly proportional to the average cluster size, provided that the pyranine content is not so high as to quench the fluorescence intensity by excitation transfer effect.

Gelation theory often makes the assumption that the conversion factor, p, alone determines the behavior of the gelation process, though p may depend on temperature, content of monomers, and time [28,29]. If the temperature and content are kept fixed, then p will be directly proportional to the reaction time, t. This proportionality is not linear over the whole range of reaction time, but it can be assumed that in the critical region, i.e. around the critical point, $|p - p_c|$ is linearly proportional to the $|t - t_{\text{gel}}|$ [33,34], where t_{gel} is defined as the gel point. Therefore, below the gel point, i.e. for $t < t_{\text{gel}}$, the maximum fluorescence intensity, $I_{\max}$, measures the weight average degree of polymers (or average cluster size). Above t_{gel}, if the intensity from finite clusters distributed through the infinite network I_{ct} is subtracted from the maximum fluorescence intensity, then, the corrected intensity $I_{\max} - I_{ct}$ measures solely the gel fraction G, the fraction of the monomers that belong to the macroscopic network. In summary, we have the following relations,

$$I_{\max} \propto DP_w = C_+\left(t_{\text{gel}} - t\right)^{-\gamma} \quad t \to t_{\text{gel}}^- \tag{8a}$$

$$I_{ct} \propto DP_w = C_-\left(t_{\text{gel}} - t\right)^{-}\gamma' \quad t \to t_{\text{gel}}^+ \tag{8b}$$

$$I_{\max} - I_{ct} \propto G = B\left(t - t_{\text{gel}}\right)^{\beta} \quad t \to t_{\text{gel}}^+ \tag{9}$$

where C_+, C_- and B are the critical amplitudes.

It is well known that the average cluster size of the finite clusters (distributed through the infinite network) above the gel point decreases with the same, but negative slope of the increasing cluster size before the gel point. This means that the exponents γ and γ', defined

for the cluster sizes below and above the gel point, have the same values [28,29,31,32]. But, the critical amplitudes for the average cluster size defined below (C_+ in Equation (8a)) and above (C_- in Equation (8b)), the gel point are different, and there exist a universal value for the ratio C_-/C_+. This ratio is different for mean-field *versus* percolation as discussed by Aharony [35] and Stauffer [28]. The estimated values for C_-/C_+ [28,35] are given in Table 1.

To determine the intensity I_{ct} in Equations (8b) and (9), we first choose the parts of the intensity–time curves up to the gel points. Then, the mirror symmetry I_{ms} of these parts, according to the axis perpendicular to time axis at the gel point was multiplied by the ratio C_-/C_+, so that $I_{ct}=\frac{C_-}{C_+}I_{ms}$. Thus, I_{ct} solely measures the intensity from the cluster above the gel point, and $I_{\max}-I_{ct}$ measures the intensity from the gel fraction.

3. Materials and methods

3.1. *Preparation of the composites*

Composite gels were prepared from SA (Alginic acid sodium salt (viscosity of 2% solution 250 cps at 25°C), Sigma) and AAm (Acrylamide, Merck) as shown in Figure 1. SA, AAm, the linear components; BIS (N,N' methylenebisacrylamide, Merck), the cross linker; APS (ammonium persulphate, Merck), the initiator; and TEMED (tetramethlethylenediamine, Merck), the accelerator were dissolved in distilled water at room temperature. AAm content was kept constant at 2 M for all solutions and SA contents changed between 0.06% and 2% (w/v). AAm and SA contents of initial solutions are given in Table 2. The initiator and pyranine (8-hydroxypyrene-1,3,6-trisulphonic acid, trisodium salt, HPTS) contents were kept constant at 7×10^{-3} and 4×10^{-4} M, respectively, for all samples.

Table 1. The estimated values for the ratio C_-/C_+ from ref. [35].

		Percolation			
	Classical	Direct ε expansion	$\gamma_{\varepsilon\exp}=1.840$ and $\beta_{\varepsilon\exp}=0.52$	$\gamma=1.7$ and $\beta=0.4$	Series and Monte Carlo
C_-/C_+	1	1/2.7	1/3.5	1/4.3	1/10

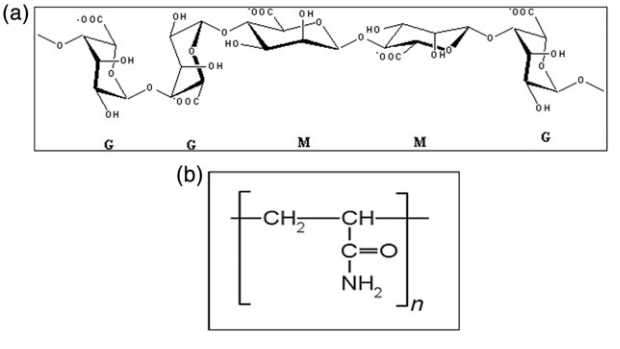

Figure 1. The chemical structures of: (a) SA [3] and (b) acrylamide.

Table 2. Experimentally measured parameters for PAAm–SA composite.

PAAm (M)	% (w/v) SA	C_-/C_+	t_{gel} (min)	β	γ
2	0.06	1.0	6	0.91	1.75
		0.37		0.66	1.66
		0.28		0.65	1.73
		0.23		0.6	1.66
		0.1		0.7	1.68
2	0.12	1.0	8	0.91	1.66
		0.37		0.58	1.66
		0.28		0.58	1.66
		0.23		0.62	1.66
		0.1		0.6	1.72
2	0.25	1.0	13	0.92	1.66
		0.37		0.62	1.62
		0.28		0.70	1.63
		0.23		0.68	1.86
		0.1		0.64	1.75
2	0.5	1.0	12	1.1	0.95
		0.37		1.0	0.95
		0.28		1.1	1.00
		0.23		0.95	1.33
		0.1		1.0	1.15
2	1	1.0	13	1.00	1.33
		0.37		1.00	1.25
		0.28		1.00	1.28
		0.23		0.88	1.28
		0.1		0.88	1.14
2	1.5	1.0	20	1.0	0.96
		0.37		1.0	0.96
		0.28		1.0	1.03
		0.23		0.98	1.06
		0.1		0.98	0.98
2	2	1.0	19	1.00	1.13
		0.37		0.93	1.15
		0.28		0.93	1.10
		0.23		0.90	1.10
		0.1		0.90	1.12

After bubbling nitrogen for 10 min, each pre-composite gel solution of 5 mL was poured into a cylindrical glass tube and put into the sample holder of the spectrometer.

3.2. *Fluorescence measurement*

The fluorescence intensity measurements during gelation were carried out using the Model LS-50 spectrometer of Perkin Elmer. All measurements were made at a 90° position and slit widths were kept at 2.5 nm. Pyranine was excited at 340 nm wavelength of light and variation in the fluorescence spectra and emission intensity of the pyranine were monitored as a function of gelation time.

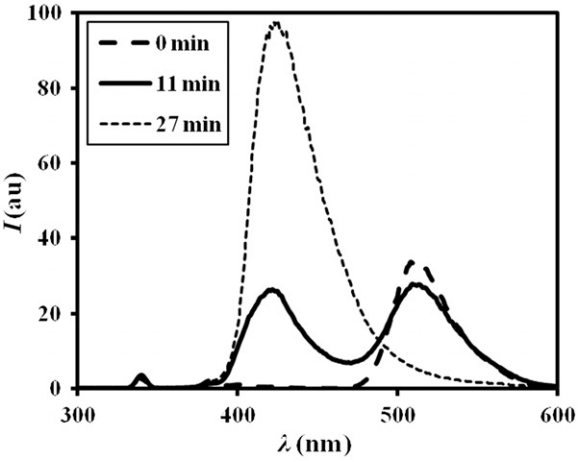

Figure 2. Fluorescence spectra of pyranine at different gelation times for 1% (w/v) SA content.

4. Results and discussion

The typical fluorescence spectra of pyranine at different stages of the AAm–SA polymerization are shown in Figure 2. At the beginning of the reaction, only the 508 nm peak, belonging to the free pyranine exists. Then, the intensity of the new (short-wavelength, around 380 nm) peak started to increase and shifted from 380 to 427 nm as the intensity of the 508 nm peak (long-wavelength peak) decreased during the course of PAAm–SA polymerization. Pyranine is a highly water-soluble compound with well-characterized photophysical properties [36]. Pyranine has three functional groups by which it can be bonded to the polymeric network, branched or linear polymers. The probability that pyranine is bonded to the system over more than one functional groups may increase with increasing polymer content, and also with the reaction time. As the polymerization progresses, pyranine can have a chance to bind the polymeric system over two or three functional groups. Here, a considerable shift from 508 to 380 nm, as previously observed [37], occurs in the emission spectra when $-$OH group in pyranine covalently binds to a vinyl group of the growing AAm and/or SA polymer chains. At the same time, shift in the short-wavelength peak from 380 to 427 nm is due to binding of SO_3^- groups on pyranine, electrostatically to the AAm and/or SA monomers with protonated amide groups whether on the same polymer molecule or on the other near polymer strands.

Figure 3(a) and (b) shows the fluorescence intensity of the 508 nm peak, I_{508nm} (corresponding to free pyranines in the composite) from the reaction mixture as a function of the reaction time for 0.12% and 1% (w/v) SA contents, respectively. As seen in Figure 3(a) and (b), the fluorescence intensity of the free pyranines first decreased, then increased up to some point, and then decreased to zero at the end of the reaction for lower SA contents (0.12% and 1% (w/v) SA).

Figure 4 shows the fluorescence intensities from the bonded pyranine against the reaction time for 0.12% and 1% (w/v) SA contents. Since the maxima of the spectra, I_{max} (corresponding to bonded pyranine), shifts from 380 to 427 nm as the polymerization has progressed, one does not have a chance to monitor the intensity in the time drive mode of the spectrometer (10 possible data in 1 s). Therefore, we monitored the fluorescence spectra in relatively large periods of time and plotted the intensity I_{max} corresponding to the

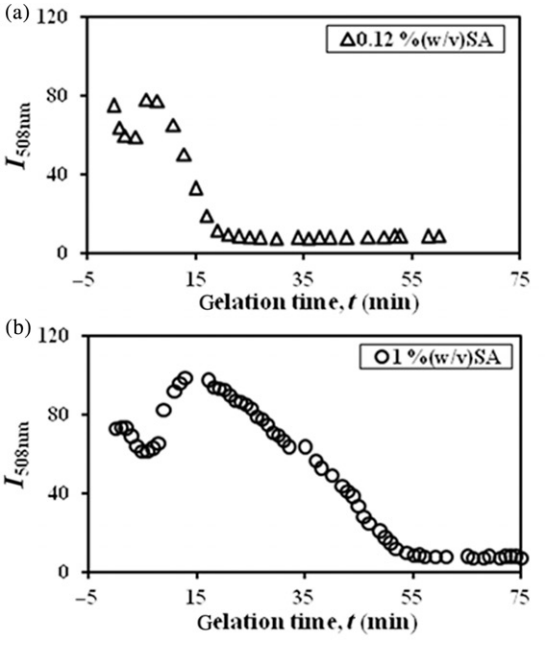

Figure 3. Fluorescence intensity of the free pyranine at 508 nm, I_{508nm}, *vs.* gelation time for: (a) 0.12% (w/v) and (b) 1% (w/v) SA contents, respectively.

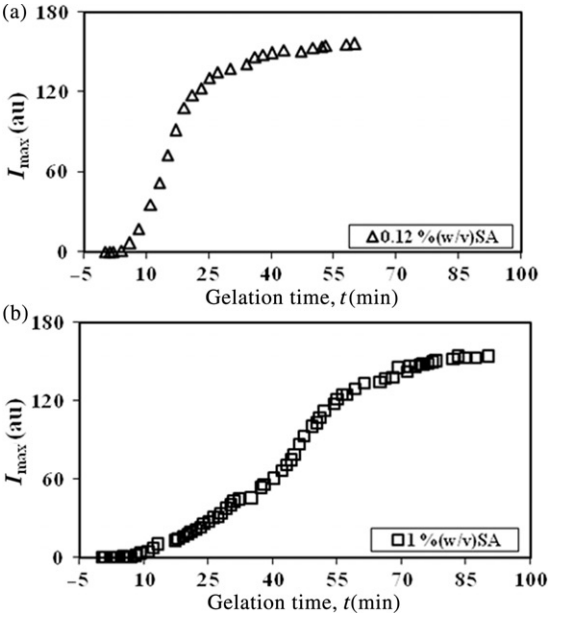

Figure 4. Fluorescence intensity variation of the bounded pyranine *vs.* gelation time for: (a) 0.12% (w/v) and (b) 1% (w/v) SA contents, respectively.

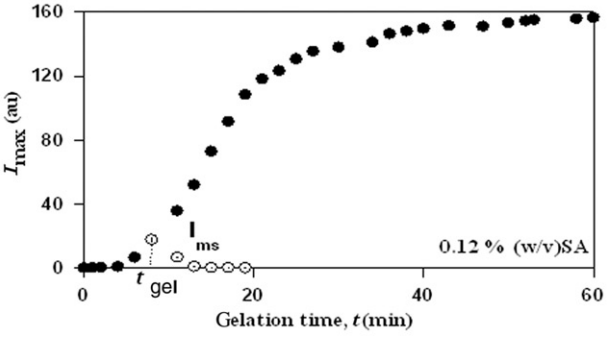

Figure 5. Intensity–time curve during occurring of PAAm-0.12% (w/v) SA composite gels. The curve depicted by dots represents the mirror symmetry I_{ms} of the intensity according to the axis perpendicular to time axis at $t = t_{gel}$. The intensity from the clusters above the gel point is calculated as $I_{ct} = \frac{C_-}{C_+} I_{ms}$. Thus, $I_{max} - I_{ct}$ monitors the growing gel fraction for $t > t_{gel}$. The intensity from the part below the symmetry axis monitors the average cluster size for $t < t_{gel}$.

maxima of the spectra as a function of time in Figure 4. We, then, used these data to evaluate the critical behavior of the sol–gel phase transition.

Figure 5 shows the intensity curve during gelation of PAAm-0.12% (w/v) SA composite gels. The curve depicted by dots represents the mirror symmetry I_{ms} of the intensity according to the axis perpendicular to time axis at $t = t_{gel.}$ The intensity from the clusters above the gel point was calculated as $I_{ct} = \frac{C_-}{C_+} I_{ms}$. Thus, the intensity below the symmetry axis monitors the average cluster size for $t < t_{gel}$, as given in Equations (8a) and (8b). $I_{max} - I_{ct}$ given in Equation (9), monitors the growing gel fraction for $t > t_{gel}$. Here, the gel point t_{gel} was determined by the dilatometric technique [38]. A steel sphere of 4.8 mm diameter was slowly moved in the composite gel up and down by means of a piece of magnet applied from the outer face of the composite cell. The time at which the motion of the sphere is stopped is called the onset of the gel point, t_{gel}. The t_{gel} values are summarized in Table 2 together with the other parameters.

Figure 6 represents the log–log plots of the typical intensity–time data below and above the gel point, t_{gel} for 1% (w/v) SA content ($C_-/C_+ = 0.1$), where the slopes of the straight lines, close to the gel points, give β and γ exponents, respectively. The produced β and γ values together with t_{gel} are listed in Table 2 for various SA contents. Here, we have to note that β and γ exponents, as seen in Table 2, strongly support that AAm–SA composites during gelation agree with the percolation picture for (<0.25% (w/v)) SA content. However, classical results were produced for (<2% (w/v)) SA contents. In other words, SA units in PAAm matrix, most probably form a percolation network (monomers are thought to occupy the sites of a periodic lattice) for (<0.25% (w/v)) SA content. On the other hand, Cayley tree structure (each bond between two monomers is randomly formed (classical)) [28], and constructed by SA units in PAAm matrix (<2% (w/v)) SA contents.

5. Conclusions

This study has presented a study of the gelation of AAm–SA composite gels where the critical exponents were determined in the view of universality. Our previous studies

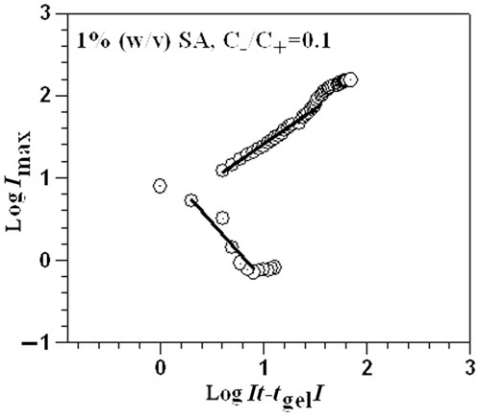

Figure 6. Double logarithmic plot of the intensity I_{max} *vs.* time curves below and above t_{gel} for 1% (w/v) SA content ($C_-/C_+ = 0.1$). The β and γ exponents were determined from the slopes of the straight lines, respectively.

showed that the produced critical exponents follow the features of different universality classes for AAm [39], PAAm-kappa(κ)-carrageenan [20], PAAm–PNIPA [21], and PAAm-MWNTs [22] composite gels. In AAm hydrogels, it was shown that the critical exponents agree best with the percolation results for high AAm contents above 1 M, but they cross over from percolation to classical (mean-field or Flory–Stockmayer) values when the AAm content goes from 2 M to lower values down to 1 M, and present classical values below 1 M. Further down, below 0.5 M, however, no gelation was observed [39]. On the other hand, in PAAm-kappa(κ)-carrageenan composite gels [20], the gel fraction exponent β agreed with the percolation result for low carrageenan contents (<2.0%). However, classical results were produced at high carrageenan content (>2.0%). On the other hand, PAAm–PNIPA and PAAm-MWNT composites show that the gel fraction exponent β obeyed the percolation result [21,22]. In this study, the critical exponents of AAm–SA composite gels were investigated for various SA contents and it was observed that the gel fraction exponent β and γ agree best with the percolation theory for (<0.25% (w/v)) SA contents. On the other hand, β and γ agreeing best with the classical (mean-field or Flory–Stockmayer) results were produced for (<2% (w/v)) SA contents. Also, critical time (gel point) was increased as a function of SA contents in PAAm–SA composite gels. We were, thus, able to measure the universality of PAAm–SA composite gels without mechanically disturbing the system. In the mean time, the universality of the sol–gel transition was tested as a function of parameters like SA contents. It is mentioned that the critical exponents did not obey the same universality class, where the most important factor is the monomer content in which the exponents drastically differ from percolation to the classical values in the composite hydrogels.

Acknowledgments

Experiments were done in the Spectroscopy Lab in the Department of Physics Engineering of Istanbul Technical University. We thank the Turkish Academy of Science (TUBA) for the partial support.

References

[1] D.J. McHugh, *A guide to the seaweed industry, FAO Fichers Technical Paper*, in *Alginate*, Vol. 441, Rome, 2003, pp. 39–49.

[2] L. Lu, X. Liu., L. Dai, and Z. Tong, *Difference in concentration dependence of relaxation critical exponent n for alginate solutions at sol-gel transition induced by calcium cations*, Biomacromolecules 6 (2005), pp. 2150–2156.

[3] T. Tripathy, S.R. Pandey., N.C. Karmakar, R.P. Bhagat, and R.P. Singh, *Novel flocculating agent based on sodium alginate and acrylamide*, Eur. Poly. J. 35 (1999), pp. 2057–2072.

[4] X. Liu, L. Qian, T. Shu, and Z. Tong, *Rheology characterization of sol-gel transition in aqueous alginate solutions induced by calcium cations through in situ release*, Polymer 44 (2003), pp. 407–412.

[5] M.G. Neumann, C.C. Schmitt, and E.T. Iamazaki, *A fluorescence study of the interations between sodium alginate and surfactants*, Carbohydr. Res. 338 (2003), pp. 1109–1113.

[6] D. Şolpan and M. Torun, *Investigation of complex formation between(sodium alginate/acrylamide) semi-interpenetrating polymer network and lead, cadmium, nickel, ions*, Colloids Surf. A: Physicochem. Eng. Aspect 268 (2005), pp. 12–18.

[7] L. Lu, X. Liu, Z. Tong, and Q. Gao, *Critical exponents and self similarity for sol-gel transition in aqueous alginate systems induced by in situ release of calcium cations*, J. Phys. Chem. B 110 (2006), pp. 25013–25020.

[8] C.M. Silva, A.J. Ribeiro, I.V. Figueiredo, A.R. Golçalves, and F. Veiga, *Alginate microspheres prepared by internal gelation: Development and effect on insulin stability*, Int. J. Pharm. 311 (2006), pp. 1–10.

[9] D. Şolpan and M. Torun, *Synthesis and characterization of sodium alginate/acrylamide semi-interpenetrating polymer networks*, J. Appl. Polym. Sci. 100 (2006), pp. 335–342.

[10] H. Omidian, J.G. Rocca, and K. Park, *Elastic, superporous hydrogel hybrids of polyacrylamide and sodium alginate*, Macromol. Biosci. 6 (2006), pp. 703–710.

[11] D. Şolpan, M. Torun, and O. Güven, *The usabiliy of (sodium alginate/acrylamide) semi-interpenetrating polymer networks on removal of some textile dyes*, J. Appl. Polym. Sci. 108 (2008), pp. 3787–3795.

[12] G.M. Barrow, *Introduction to Molecular Spectroscopy*, McGraw-Hill, New York, NY, 1962.

[13] J.B. Birks, *Photopyhsics of Aromatic Molecules*, Wiley, Interscience, New York, NY, 1971.

[14] D.M. Herculus, *Fluorescence and Phoshoperence Analysis*, Wiley Intersicence, New York, NY, 1965.

[15] W.F. Jager, A.A. Volkers, and D.C. Neckers, *Solvatochromic fluorescent probes for monitoring the photopolymerization of dimethacrylates*, Macromolecules 28 (1995), pp. 8153–8158.

[16] T.C. Schaeken and J.M. Warman, *Radiation-induced polymerization of a mono- and diacrylate studied using a fluorescent molecular probe*, J. Phys. Chem. 99 (1995), pp. 6145–6151.

[17] J.S. Royal and J.M. Torkelson, *Physical aging effects on molecular-scale polymer relaxations monitored with mobility-sensitive fluorescent molecules*, Macromolecules 26 (1993), pp. 5331–5335.

[18] K.E. Miller, R.H. Krueger, and J.M. Torkelson, *Mobility-sensitive fluorescence probes for quantative monitoring of water sorption and diffusion in polymer coatings*, J. Polym. Sci., Part B: Polym. Phys. 33 (1995), pp. 2343–2349.

[19] R. Vatanparast, S. Li, K. Hakala, and H. Lemmetyinen, *Monitoring of curing of polyurethane polymers with fluorescence method*, Macromolecules 33 (2000), pp. 438–443.

[20] D. Kaya Aktaş, G.A. Evingur, and Ö. Pekcan, *Universal behaviour of gel formation from acrylamide-carrageenan mixture around the gel point: A fluorescence study*, J. Biomol. Struct. Dyn. 24(1) (2006), pp. 83–90.

[21] G. Akın Evingur, D.K. Aktas, and Ö. Pekcan, *Steady state fluorescence technique for studying phase transitions in PAAm- PNIPA mixture*, Phase Transitions 82(1) (2009), pp. 53–65.

[22] D.K. Aktaş, G.A. Evingur, and Ö. Pekcan, *Critical exponents of gelation and conductivity in Polyacrylamide gels doped by multiwalled carbon nanotubes*, Compos. Interfaces 17 (2010), pp. 301–318.

[23] P.J. Flory, *Molecular size distribution in three dimensional polymers. I. Gelation*, J. Am. Chem. Soc. 63 (1941), pp. 3083–3090.
[24] P.J. Flory, *Molecular size distribution in three dimensional polymers. II. Trifunctional branching units*, J. Am. Chem. Soc. 63 (1941), pp. 3091–3096.
[25] P.J. Flory, *Molecular size distribution in three dimensional polymers. III. Tetrafunctional branching units*, J. Am. Chem. Soc. 63 (1941), pp. 3096–3100.
[26] W. Stockmayer, *Theory of molecular size distribution and gel formation in branched-chain polymers*, J. Chem. Phys. 11 (1943), pp. 45–54.
[27] W. Stockmayer, *Theory of molecular size distribution and gel formation in branched polymers II. General cross linking*, J. Chem. Phys. 12 (1944), pp. 125–129.
[28] D. Stauffer, A. Coniglio, and M. Adam, *Gelation and critical phenomena*, Adv. Polym. Sci. 44 (1982), pp. 103–158.
[29] D. Stauffer and A. Aharony, *Introduction to Percolation Theory*, 2nd ed., Taylor and Francis, London, 1994.
[30] C.P. Lusignan, T.H. Mourey, J.C. Wilson, and R.H. Colby, *Viscoelasticity of randomly branched polymers in the vulcanization class*, Phys. Rev. E: Stat. Nonlinear Soft Matter Phys. 60 (1999), pp. 5657–5669.
[31] M. Sahimi, *Application of Percolation Theory*, Taylor and Francis, London, 1994.
[32] P.G. de Gennes, *Scaling Concepts in Polymer Physics*, Cornell University Press, Ithaca, NY, 1979.
[33] Y. Yilmaz, A. Erzan, and Ö. Pekcan, *Critical exponents and fractal dimension at the sol- gel phase transition via in situ fluorescence experiments*, Phys. Rev. E: Stat. Nonlinear Soft Matter Phys. 58 (1998), pp. 7487–7491.
[34] Y. Yilmaz, A. Erzan, and Ö. Pekcan, *Slow release percolate near glass transition*, Eur. Phys. J. E 9 (2002), pp. 135–141.
[35] A. Aharony, *Universal critical amplitude ratios for percolation*, Phys. Rev. B: Condens. Matter 22 (1980), pp. 400–414.
[36] M. Ashokkumar and F. Grieser, *Sonophotoluminesans: Pyranine emission induced by ultrasound*, J. Chem. Soc. Chem. Commun. (1998), pp. 561–562.
[37] Y. Yilmaz, N. Uysal, A. Gelir, O. Güney, D.K. Aktaş, S. Göğebakan, and A. Öner, *Elucidation of multiple-point interactions of pyranine fluoroprobe during the gelation*, Spectrochimica Acta A Mol. Biomol. Spectrosc. 72 (2009), pp. 332–338.
[38] O. Okay, D. Kaya, and Ö. Pekcan, *Free-radical crosslinking copolymerization of styrene and divinylbenzene: Real time monitoring of the gel effect using fluorescence probe*, Polymer 40 (1999), pp. 6179–6187.
[39] D. Kaya, Ö. Pekcan, and Y. Yılmaz, *Direct test of the critical exponents at the sol- gel transition*, Phys. Rev. E: Stat. Nonlinear Soft Matter Phys. 69 (2004), p. 016117(1–10).